NBSIR 75-787

Piezo- and Pyroelectric Properties of Electrets

Martin G. Broadhurst and G. Thomas Davis

Institute for Materials Research
National Bureau of Standards
Washington, D. C. 20234

October 1975

Final - January 1, 1975 - December 31, 1975

NBSIR 75-787

PIEZO- AND PYROELECTRIC
PROPERTIES OF ELECTRETA

Martin G. Broadhurst and G. Thomas Davis

Institute for Materials Research
National Bureau of Standards
Washington, D. C. 20234

October 1975

Final - January 1, 1975 - December 31, 1975

4. PIEZO- AND PYROELECTRIC PROPERTIES

M. G. Broadhurst and G. T. Davis
National Bureau of Standards
Washington, D. C. 20234

4. Piezoelectric and Pyroelectric Properties

Introduction

Oliver Heavside [4.1] in 1892, postulated that certain waxes would form permanently polarized dielectrics when allowed to solidify from the molten state in the presence of an electric field. He viewed an electret as the electrical analog of a magnet, that is, as having a frozen-in, relatively long lived (compared to the observation time) non-equilibrium electric dipole moment. Present popular usage has expanded this concept of an electret to include monopolar dielectrics having a net frozen-in real charge. For example, the commercial electret microphone employs a monopolar polymer film. Wax and rosin electrets were made and studied by EGUCHI in the early 1920's [4.2].

It was well understood by 1927 [4.3] that molecules containing permanent electric moments orient in the direction of an electric field when mobile in the liquid state. Upon solidification of the material in the presence of the field, the dipoles lose their mobility while retaining their preferred orientation. The net dipole orientation produces the electret's permanent polarization (net dipole moment per unit volume). It was also recognized that in addition to the electret's moment there were also real charges, generally concentrated near the electret surfaces, which were injected during the formation process by field emission, gas breakdown or similar processes.

In 1927 piezoelectricity and pyroelectricity were shown theoretically and experimentally to be properties exhibited by electrets with preferentially ordered dipoles [4.3, 4]. However, these early wax electrets had poor mechanical strength and low sensitivity, and applications for them did not develop. More recently, strong, highly active polymer films, notably poly(vinylidenefluoride), PVF_2, poly(vinylfluoride), PVF, and poly(vinylchloride), PVC, have been recognized for their potential value as thermoelectric and thermomechanical transducer materials. Already these materials are finding their way into a new technology

of polymer transducers. Japanese scientists have been particularly active in
the early research and development of these devices with the work of FUKADA on
natural and synthetic polymers [4.5], KAWAI who pointed out how general the
effect is [4.6], HAYAKAWA and WADA with their theoretical analyses [4.7] and
industrial scientists who are developing films [4.8, 9] and using them for
various devices [4.10-12]. Most of the polymer electret work in the U.S. has
focused on using the pyroelectric response for electromagnetic radiation detection
[4.13-21].

In the following sections we shall present concepts, models, experimental
considerations, results, and implications which have resulted from some of the
work on piezoelectric and pyroelectric polymers. This approach is intended to
provide the reader with basic physical concepts needed to identify important
molecular and material parameters, deduce guide-lines for optimizing desirable
properties and provide a basis for selecting new applications.

4.1 Thermodynamic Definitions

Piezo- and pyroelectricity are defined in a formal way by thermodynamics
[4.22]. The piezoelectric constant d_{mj}, is a tensor component given by a second
derivative of the Gibbs free energy with respect to the electric field vector
$\underline{E}$ and stress tensor $\underline{T}$.

$$d_{mj} = \left[\frac{\partial^2 G(\underline{E}, \underline{T}, T)}{\partial E_m \partial T_j} \right] T \qquad (4.1)$$

We define a material as being piezoelectric if this second derivative has a
value large enough to be measurable. A material is pyroelectric if at least one
of the components of the pyroelectric coefficient vector $\underline{p}$ defined as

$$P_m = \left[\frac{\partial^2 G(\underline{E}, \underline{T}, T)}{\partial E_m \partial T} \right] \underline{T} \qquad (4.2)$$

has a value large enough to be measurable. Being second derivatives of free

energy, these coefficients have a basis in common with better known quantities

such as coefficients of expansion, compressibility, heat capacity and dielectric

constant and can therefore be expected to be complex quantities if measured

with an alternating stress or show relaxational behavior in the time domain.

The second derivatives in (4.1) and (4.2) can be taken in any order so that

we have,

$$d_{mj} = (\partial D_m / \partial T_j)_{T,\underline{E}} = (\partial S_j / \partial E_m)_{\underline{T},\ T} \tag{4.3}$$

and

$$p_m = (\partial D_m / \partial T)_{\underline{E}} = (\partial \Sigma / \partial E_m)_T \tag{4.4}$$

In the above, j=1,...6; m=1, 2, 3; $\underline{T}$=stress; S=strain; D=electric displacement;

E=electric field; T=temperature; Σ=entropy.

The d are often called piezoelectric strain constants whereas the piezo-

electric stress constants, e, arise from taking S rather than $\underline{T}$ as the independent

variable in (4.1).

Two other piezoelectric constants h and g can be defined by taking D and

S and D and $\underline{T}$ as independent variables in (4.1), [4.23]. Before relating the

quantities defined in (4.3) and (4.4) to measured quantities, it is well to

develop a better description of an electret and understand the influence of

real and dipolar charges.

4.2 Physical Description of an Electret

4.2.1 Preparation

Consider a slab of polymer which we take to be amorphous, homogeneous,

and elastically isotropic. We first evaporate metallic electrodes on both

sides to eliminate air gaps between the polymer and metal, and then follow the

- 4 -

temperature-voltage-time sequence shown schematically in Fig. 4.1: 1) raise

the temperature from room temperature T_r to an elevated temperature which we

show here as being above the glass transition temperature, T_g; 2) apply a dc

voltage, Φ of a few kilovolts resulting in an electric field of several hundred

kilovolts per centimeter of slab thickness, s, between the electrodes; 3) while

maintaining this voltage, lower the temperature back to T_r. The electret thus

formed can be represented schematically as shown in Fig. 4.2.

The above poling procedure typically introduces both real and dipolar

charges, and these will affect the behavior of the electret in different ways.

To explain this difference we will consider the two types of charge separately.

4.2.2 Real Charges - Monopolar Electrets

In general, real charges do not contribute to a piezo- and pyroelectric

response as long as the sample is strained uniformly [Ref.4.7, Sec. 2.2]. To

illustrate this fact, consider the example of Fig. 4.3. A slab of dielectric

with relative permittivity κ, thickness s and short circuited contact electrodes

contains a layer of trapped positive charges at a distance, x, from the bottom

electrode. The charge densities on the bottom and top electrodes are σ_o and σ_s

and the charge density of the trapped charge is σ_x. Using Gauss' theorem to

calculate the field due to a plane of charge, the difference between the surface

charge densities on the two electrodes, $\Delta\sigma$, is

$$\Delta\sigma = \sigma_o - \sigma_s = \sigma_x (1 - 2x/s) \qquad (4.5)$$

If the material is strained so that the distances x and s change to x + Δx and

s + Δs, then the difference in surface charge $\Delta\sigma$ becomes:

$$\Delta\sigma = \sigma_x[1 - 2(x + \Delta x)/(s + \Delta s)] = \sigma_x[1 -(2x/s)(1 + \Delta x/x)/(1 + \Delta s/s)] \qquad (4.6)$$

If the strain is uniform so that $\Delta x / x = \Delta s / s$ then $\Delta \sigma' = \Delta \sigma$ and no charge will flow as a result of pressure and temperature changes which produce the strain. This result has been experimentally verified in our laboratory by measurements on electron-beam-irradiated, fluorinated ethylene-propylene copolymers and by measurements on samples at varying times after poling when their real charge content was decaying rapidly. In neither case was there a significant piezo- and pyroelectric response attributable to real charge.

Although the homogeneous monopolar electret is generally not piezo- or pyroelectric it still has considerable value in transducer devices such as strain sensitive cables and electret microphones. We will describe this effect in order to clarify the distinction between it and a dipolar electret behavior.

Figure 4.4 shows a schematic diagram of a polymer film which contains real charges trapped in the polymer matrix (monopolar electret). The film is mounted so that an air gap separates it from a conductive plate. As the charged film moves with respect to the plate (under the influence of sound waves, for example) the plate potential changes and charges flow between it and a conductive contact electrode on the film through an appropriate circuit. A good polymer for these devices is fluorinated ethylene-propylene copolymer [4.24, 25]. This same effect is probably a source of electrical signals generated in flexible polymer-insulated coaxial cable when it is subjected to mechanical vibrations or pressure changes. Note that the electret microphone system does not undergo uniform strain. That is, the air gap is strained much more than the polymer film and hence the real charges do contribute to current flow. This result suggests the possibility that artificial piezoelectrics could be made from alternate layers of material of different compressibility with appropriate charges trapped at the interfaces. It has been proposed that such a mechanism may be responsible for piezoelectricity in polyvinylidene fluoride, as will be discussed in Subsect. 4.5.4.

4.2.3 Dipolar Electret

To illustrate the electret's piezoelectric and pyroelectric behavior consider Fig. 4.5 and 4.6. As the electrically short-circuited electret contracts due to an increase in hydrostatic pressure or a decrease in temperature the metal electrodes move closer to the dipoles and the zero potential is maintained by a flow of charge. This model of a strain sensitive electret is similar to that given by Adams [4.3] and accounts for most of the response of piezoelectric and pyroelectric polymers. Note that the model predicts the direction of current flow in terms of the direction of the poling field and also predicts that while the total charge released is proportional to the temperature or pressure change, the current depends on the rate of pressure or temperature change and can be quite large. This effect can be described mathematically as follows.

In terms of the material's relative permittivity κ' the equilibrium field-induced polarization is given by,

$$P = (\kappa' - 1) \, \varepsilon_o E \tag{4.7}$$

where ε_o is the permittivity of vacuum and E is the applied field. In the molecularly mobile liquid phase the field produces a polarization

$$P_L (T) = (\kappa_L (T) - 1) \, \varepsilon_o E_P \tag{4.8}$$

where the subscript L refers to the liquid phase,(T) to the functional dependence on temperature and $E_P = \phi/s$ is the nominal poling field. During poling, the field maintains this polarization while the temperature is lowered enough to immobilize the molecular dipoles. The field is removed and the lost polarization (neglecting volume change) is,

$$P_s (T) = (\kappa_s (T) - 1) \, \varepsilon_o E_P, \tag{4.9}$$

where the subscript s refers to the solid phase.

Thus the frozen-in non-equilibrium polarization remaining after removal of the poling field is:

$$P_o (T) = (\kappa_L (T_L) - \kappa_s (T)) \varepsilon_o E_P \qquad (4.10)$$

where T_L is the temperature where the material becomes liquid. Eq. (4.10) provides a method of calculating the frozen dipole polarization for linear dielectrics from a knowledge of their relative permittivity at the polar and measuring temperatures. In order to calculate the piezoelectric and pyroelectric coefficients from molecular properties one needs to use a more detailed model as shown below.

The polarization (dipole moment per unit volume) is defined as

$$N <m>/V \qquad (4.11)$$

where N is the number of dipoles, V the volume of the electret and <m> the mean effective dipole moment in the direction of P. As a model for the electret with preferentially ordered polarizable dipoles of permanent moment μ_o, consider Fig. 4.7 One can use an Onsager type calculation [4.26] to determine the effective moment <m> in Eq. (4.11) of a representative dipole located in a spherical cavity and oriented at a fixed average angle θ with respect to the direction of overall polarization P. Such a calculation leads to the result [4.27]:

$$P_o = (\kappa_\infty + 2) N \mu_o <\cos \theta>/3V \qquad (4.12)$$

where κ_∞ is the high frequency relative permittivity related to the polarizability through the Clausius-Mosotti relationship and N/V is the number of dipoles per unit volume. This important equation can be used to calculate the piezo- and

pyroelectric coefficients for this model. This calculation is done simply by taking the derivatives of P_o with respect to pressure and temperature and then expressing the relationship between these derivatives and the defined quantities (4.3) and (4.4).

The relationship between P_o of Eq. (4.12) and electric displacement is given by

$$D = \kappa' \epsilon_o E + P_o \tag{4.13}$$

In the simplest case where the short-circuit current is measured while temperature or stress are changed, one obtains:

$$\frac{\partial D}{\partial T}\bigg|_{E=0,\underline{T}} = \frac{\partial P_o}{\partial T}\bigg|_{E=0,\underline{T}} = \frac{\partial (Q/A)}{\partial T}\bigg|_{E=0,\underline{T}} \tag{4.14}$$

and

$$\frac{\partial D}{\partial \underline{T}}\bigg|_{E=0,T} = \frac{\partial P_o}{\partial \underline{T}}\bigg|_{E=0,T} = \frac{\partial (Q/A)}{\partial \underline{T}}\bigg|_{E=0,T} \tag{4.15}$$

where Q/A is the surface charge per unit area of electrode. Here we continue to neglect changes in (Q/A) due to real charges.

Generally it is not a change in (Q/A) which is measured but rather a change in Q. Reported values for piezo- and pyroelectric coefficients are thus in error as far as the strict definitions are concerned. In the following we adopt common practice and redefine (4.3) and (4.4) as,

$$d = (1/A) \ (\partial Q/\partial \underline{T})_{E=0,T} \tag{4.16}$$

and

$$p = (1/A) \ (\partial Q/\partial T)_{E=0,\underline{T}} \tag{4.17}$$

The above distinction becomes particularly significant for polymers where the difference between (4.14) and (4.16) is of the order of magnitude of the terms themselves. Inorganic materials have a much smaller temperature and stress-induced area change and the corresponding difference between (4.14) and (4.16) or (4.15) and (4.17) is small.

Another inconsistency is sometimes encountered when measurements are reported at voltages considerably greater than zero. Allowing X to represent stress or temperature, the derivative,

$$\frac{\partial D}{\partial X}\bigg|_E = \frac{\partial \kappa'}{\partial X}\bigg|_E \varepsilon_o E + \kappa' \varepsilon_o \frac{\partial E}{\partial X} + \frac{\partial P_o}{\partial X}\bigg|_E \tag{4.18}$$

has two terms in addition to that in (4.14) and (4.15). The first term involving electrostriction can be large if E is large. From (4.3) and (4.4) this is a legitimate part of p and d which are functions of E. The second term would not appear if E were held constant, but in practice it is the voltage Φ that is held constant and the thickness $s = \Phi/E$ varies with the measurement and gives an electromechanical contribution. Similarly the third term is measured at constant Φ. (Electrostriction and electromechanical contributions are considered in a different way in Ref. [4.30]).

To reduce ambiguity, we will consider measurements made at zero field and for simplicity and a more straight forward comparison of p and d, will use hydrostatic pressure as mechanical stress (positive pressure is a negative stress). Without giving the details, [4.27], the straight-forward differentiation of Eq. (4.12) to obtain the pressure and temperature induced currents in an

electret gives:

$$A^{-1}(\partial Q/\partial T)_p = - P_o\ \alpha(\kappa_\infty + \phi^2/2\alpha T + 3\gamma\phi^2) \tag{4.19}$$

$$A^{-1}(\partial Q/\partial p)_T = P_o\ \beta(\kappa_\infty + 3\gamma\phi^2) \tag{4.20}$$

where $\alpha = (3V)^{-1}\ dV/dT$ is the linear coefficient of expansion, $\beta = -(3V)^{-1}\ dV/dp$ is the linear compressibility, $\gamma = V\omega^{-1}\ d\omega/dV$, is a Gruneisen constant for the dipole torsional frequency ω and ϕ^2 is the mean squared torsional displacement of dipole fluctuations.

These equations show that for this model most of the piezo- and pyroelectric response comes from volume expansion and its effect on κ_∞. There is an additional contribution from temperature change which can be illustrated with a physical model like that in Fig. 4.8. Although the dipoles have a fixed mean direction, there is always thermal motion whose mean squared amplitude in the simple harmonic approximation is proportional to temperature. Thus increasing the temperature of a dipole reduces the average magnitude of its moment. This effect was the basis of a theory of pyroelectricity in PVF_2 due to ASLAKSEN [4.28], and accounts for about 1/3 of the pyroelectricity in PVC and possibly a similar fraction in other polymers. The amplitude of molecular librations is difficult to measure or to predict *a priori* because of the large number of vibrational modes and molecular conformations contributing. However, one recent paper gives a value of 10° for the root mean squared torsional displacement of polyethylene molecules based on x-ray data [4.29].

4.3 Symmetry and Tensor Components

Crystal symmetry is usually considered in discussions of piezoelectricity. An isotropic amorphous material could not be expected to be either piezo- or pyroelectric because its response to stress will be the same in all directions.

However, if one preferentially aligns molecular dipoles in the specimen, there is an axis of symmetry in the direction of the net moment and the sample will be both piezoelectric and pyroelectric. Often, polymer films are uniaxially stretched to preferentially align the polymer molecules parallel to the stretch direction and they are then poled to align the dipoles normal to both the stretch direction and the plane of the film. (We consider only those polymers with dipoles normal to the molecular axis). The result is to destroy the axis of symmetry present in the unstretched specimen. The axes are usually identified as shown in Fig. 4.9. The expected components of the piezoelectric tensors for such a specimen and their proper signs are:

$$\underset{\sim}{d} = \begin{pmatrix} 0 & 0 & 0 & 0 & d^+_{15} & 0 \\ 0 & 0 & 0 & d^+_{24} & 0 & 0 \\ d^+_{31} & d^+_{32} & d^-_{33} & 0 & 0 & 0 \end{pmatrix} \tag{4.21}$$

$$\underset{\sim}{p} = \begin{pmatrix} 0 \\ 0 \\ p^-_3 \end{pmatrix} \tag{4.22}$$

The assignments can be made by inspection from Fig. 4.9. Stress in the + 3 direction will increase the sample thickness and thus decrease the polarization giving a negative d_{33}. The stress in the 1 and 2 directions will decrease the thickness and increase polarization, giving a positive d_{31} and d_{32}. Experimentally, d_{33} is found to be negative for PVF$_2$ [4.16] and d_{31} positive for PVF [4.31] and predominently positive for PVF$_2$ [4.16]. d was also found to be negative with hydrostatic stress for PVC [4.33]. (Remember that we are using the assumption that the electrodes expand with the specimens and that we have adopted equations (4.16) and (4.17) as our definitions. If we use the proper

definitions given by equations (4.14) and (4.15) stress in all three directions 1, 2, and 3, will increase the volume and decrease the polarization giving negative d_{3j} components). The shear components result because a positive shear about the 1 axis, T_4, rotates the dipoles into the + 2 direction and a shear about the 2 axis, T_5, rotates the dipoles into the + 1 direction. Neither shear causes a change to first order in the moment in the 3 direction. A shear about the 3 axis, T_6, does not change the moment. Because there is no net moment along the 1 and 2 axes, $p_1 = p_2 = 0$ and an increase in temperature produces an increase in volume and decrease in polarization yielding a negative p_3. The $\underset{\sim}{d}$ matrix constructed from physical arguments for amorphous polymers is characteristic of C_{2V} symmetry. This same symmetry is found for the polar crystal phase of PVF_2 [4.31] and the same crystal structure is reported for polar PVF [4.32]. Poled, unoriented polymers should give $d_{31} = d_{32}$ and $d_{24} = + d_{15}$ characteristics of a piezoelectric matrix with $C_{\infty V}$ symmetry [Ref. 4.5, Sect. IA].

4.4 Structure

4.4.1 General

Using the model discussed above it is possible to hypothesize three requirements for piezo- and pyroelectricity in polymers. i) There must be molecular dipoles present, the higher their moment and concentration the better. ii) There must be some way of aligning the dipoles, the more alignment the better. iii) There must be a way of locking-in the dipole alignment once it is achieved, the more stable the better. Evaluating these conditions for a particular polymer requires considerable data on the molecular and bulk structure and properties. In the following discussion we consider in some detail two different types of polymers--amorphous and semi-crystalline. Other types--notably the biopolymers-- will not be considered.

The polymers we will be discussing consist of a saturated carbon backbone with various combinations of fluorine, chlorine and hydrogen. The abbreviations to be used for the repeating monomer units are defined in Table 4.1 which refers to Fig. 4.10. A repeat unit consists of two carbon atoms and conformations are allowed by rotations of $2\pi/3$ rad. about carbon-carbon bonds.

4.4.2 Amorphous Polymers

PVC is an example of an amorphous polymer which can be made piezo- and pyroelectric [4.6, 33-35]. The repeat unit is polar with an effective dipole moment of 3.6×10^{-30} C·m (1.1 D) [4.36]. The usual form of PVC is amorphous because of the irregular positioning of Cl between sites 3 and 4 (Fig. 4.10). More stereo-regular (syndiotactic) crystallizable PVC can be made and its crystal structure has been determined [4.37]. PVC is an equilibrium liquid above its glass transition temperature (about 80°C) although thermal decomposition is appreciable above this temperature. Below 80°C, the kinetics of molecular reorganization are slow enough that a non-equilibrium amorphous solid (glass) is formed. Structural relaxation times of the glass increase rapidly with decreasing temperatures to the order of years at room temperature. Thus this polymer fits all criteria in 4.4.1 for piezo- and pyroelectricity. To illustrate the calculation of p and d we rewrite (4.19) and (4.20) to account for the fact that the dipoles are small enough that the product of their moment times the field is much less than their thermal energy kT and (4.10) will be valid. For more background see [Ref. 4.38, p.32].

$$p = -\Delta\kappa'\varepsilon_o E_p \alpha \left[\kappa_\infty + \phi^2/2\alpha T + 3\gamma\phi^2\right] \qquad (4.23)$$

$$d = -\Delta\kappa'\varepsilon_o E_p \beta \left[\kappa_\infty + 3\gamma\phi^2\right] \qquad (4.24)$$

We use $\Delta\kappa' = 10$ and $\kappa_\infty = 3$ [4.36], $\alpha = 0.78 \times 10^{-4}$/K, $\beta = 0.86 \times 10^{-10} m^2$/N [4.33], T = 300 K and $\phi^2 = 0.07$ rad. (from estimate of $\phi = 15°$). The Grüneisen constant is expected to be small because the force constants for dipole rotation are mostly intramolecular and do not depend strongly on volume. Neglecting the terms in γ, we find $p = -0.10$ nC/cm$^2 \cdot$ K and d = -0.73 pC/N when $E_p = 320$ kV/cm, in good agreement with measured values [4.39].

Even if one does not have dielectric data, the quantity $\Delta\kappa'$ can be calculated with reasonable confidence from the dipole moment using Onsager's equation [4.36]. REDDISH [4.36] interpreted the dielectric data on PVC as indicating that the length of the relaxing segments increased as the temperature decreased below T_g and since the $\Delta\kappa'$ increases linearly with the number of dipoles per rigid unit, large polarizations could be achieved. Unfortunately, we found no enhancement of p and d by lower temperature poling of PVC and suspect the observed effects in dielectric properties are due to space charge.

Since most of the variables in (4.23) and (4.24) will be similar for all polymer glasses, larger coefficients can be sought from polymers with a large dipole moment (p and d will increase as the square of the dipole moment per unit volume) and by increasing the poling field. A possible candidate is PAN with a dipole moment greater than 4D. Unfortunately PAN may have an anomalous liquid phase in which dipole-dipole forces prevent normal polarization [4.40] contrary to criteria (ii) in Subsect. 4.4.1. In other cases the dipoles may not become immobile at T_g (e.g. polymethylmethacrylate) contrary to criteria (iii)). A thermally stable, high T_g polar glass may have useful high temperature applications, but presently the most sensitive piezo- and pyroelectric polymers are semicrystalline.

4.4.3 Semicrystalline Polymers

The most interesting of the semicrystalline polymers are PVF_2 and PVF.
These polymers crystallize because the fluorines, unlike the large chlorines,
are close enough in size to hydrogen so as not to interfere with regular packing.
Both polymers have head-head and tail-tail defects, where successive repeat
units are backwards. These amount to 5% for PVF_2 [4.41-43] and 25-32% for PVF
[4.41]. A h-h unit in PVF_2 is immediately followed by a t-t unit [4.41] so
that 5% of these defects cancel 10% of the dipole moment of the planar zig-zag
chain. The dipole moment of a PVF_2 repeat unit can be estimated from the
average of those for difluoroethane and difluoromethane [4.44] at 7.06×10^{-30} c·m.
(2.12D). The moment for PVF in the plane of the trans planar C-C zig-zag will
be very close to 1/2 that of PVF_2, but 30% h-h defects will reduce the net
moment of the planar PVF molecule by 60%. Both of these polymers have good
thermal and chemical stability.

Semicrystalline polymers consist of lamellar crystals mixed with amorphous
regions. A schematic diagram of a semicrystalline polymer is shown in Fig. 4.11
for a low and high density sample. Annealing or crystallizing for longer times,
at higher temperatures and pressures increases the lamellar thickness and
perfection which results in a higher sample density. The crystals grow in the
form of spherulites and studies on the morphology of PVF_2 show that three crystal
phases have distinct morphology and can grow simultaneously from the melt or one
phase can grow at the expense of another [4.45]. A typical molecular weight
for these polymers is 10^5 for an extended length of 50×10^{-8}m and a total of
2000 repeat units. Since the lamellae are of the order of 10^{-8}m thick, a single

molecule folds back and forth through the lamellae many times. When stretched

to several times the original length, the specimen becomes oriented such that

the lamellae are normal to the stretch direction and the molecules are parallel

to the stretch direction [4.46-47]. PVF and PVF_2 are of the order of 50%

crystalline.

The dispersed amorphous phase seems to have normal equilibrium liquid

properties with a liquid-glass transition region around -50°C, and a WLF-type

dielectric relaxational behavior [4.17, 48, 49]. Broad line NMR [4.48, 50],

and mechanical relaxation data [4.5, 31, 42, 50, 51] also show a normal liquid-

glass relaxation. The magnitude of the dielectric dispersion and room temperature

relative permittivity increase with amorphous content as expected [4.49, 50].

From criteria (iii) in Subsect. 4.4.1 we do not expect the amorphous phase to

contribute to piezo- and pyroelectricity. MURAYAMA [4.8] has stated the same

conclusion.

Three crystal phases have been reported for PVF_2. Form β and γ (alternatively

forms I and III) are similar in that the molecules assume a planar zig-zag con-

formation and pack in the crystal with dipole moments parallel. The α form

(Form II) is in a trans-gauche-trans-gauche' conformation which is a polar

molecular configuration but which packs to form an antipolar crystal. Projections

of the α and the β and γ crystals onto a plane normal to the molecular axes are

shown in Fig. 4.12, [4.52]. The crystal structure of PVF is the same as β phase

PVF_2 [4.32]. Vibrational analyses of the proposed structures [4.52, 53] have been

done to make detailed assignments of the spectral absorptions in PVF_2. Crystal

melting points range from 230°C for PVF [4.54] to around 190°C for PVF_2 γ phase,

180°C for PVF_2 β phase and 170°C for PVF_2 α phase [4.45]. Crystallization

from the melt at lower temperatures produces α phase and at higher temperatures

γ phase [4.45, 55]. The β comes from stretching or rolling α or γ phase material

[4.52]. The γ phase can also be cast from certain solvents [4.52]. Mixtures

and copolymers of PVF and PVF_2 tend to stabilize the polar crystal form [4.54].

Model calculations of the effects of VF_2, VF, and TFE repeat units copolymerized

with PVF_2 indicate the β phase becomes stable above a 5-10% concentration of

these substituents [4.56] which has also been shown experimentally [4.57]. Work

in our laboratory has been done on a copolymer of 73% VF_2 and 27% TFE [4.58] which

is completely β phase in accord with the above prediction [4.56]. Copolymers of

VF_2, VF and TFE can be highly piezo- and pyroelectric [4.9].

The usual methods of identifying the fraction of crystallinity in a specimen

are to compare its density to the crystal and amorphous densities [4.59] or to

compare its heat of fusion to the crystalline heat of fusion [4.45]. The usual

measures of crystal phase fractions are x-ray diffraction [4.60] and infra-red

absorption [4.55] intensity ratios.

4.5 Properties of Semicrystalline Polymers

4.5.1 Crystal Relaxations

In the crystal phases of PVF and PVF_2 the question of rotational freedom

of the dipoles is critical [Subsect. 4.4.1, ii]. Ample dielectric relaxation

data exist on PVF [4.61] and α phase PVF_2 [4.17, 49, 59, 61-64] and mechanical

data on PVF [4.51] and α phase PVF_2 [4.50] and thermally stimulated current (TSC) data

on α phase PVF_2 [4.17] to conclude that a crystal relaxation α_c occurs at about

80°C at a measuring frequency of 100 Hz. At room temperature the relaxation

time τ_c of the α_c relaxation is increased to about 1 sec. Log τ_c is linear with

1/T and the activation energy is around 100 kJ/mol. The β phase of PVF_2 is reported to have a mechanical crystal relaxation at 110°C at 10 Hz [4.31, 50]. Its activation energy has not been determined. A dielectric a_c relaxation in β and γ phase PVF_2 have yet to be clearly observed, but may be masked by rapidly increasing κ' and κ'' with temperature. This behavior is usually attributed to space charge effects [4.61, 63, 64]. TSC data give strong background currents even from unpoled specimens [4.11]. At lower temperatures current with a broad maximum at 80° and integrated charge of up to 3 $\mu C/cm^2$ is observed [4.20]. It is useful to infer the behavior of the α_c relaxation in β and γ PVF_2 from that in α phase PVF_2, PVF and PE. That the dielectric α_c is a crystal relaxation was shown for α phase PVF_2 by the dependence of its amplitude on crystallinity and by observing its disappearance at the melting temperature [4.49]. That it can exist in the β phase is demonstrated by its presence in PVF [4.61]. That it probably involves rotation of an entire intralamellar segment with twisting at the lamellae surfaces is likely considering that this is the well documented α_c mechanism in PE [4.65]. Since twisting must be about C-C bonds, these rotations would be restricted by the crystal fields of neighboring molecules. This model is also consistent with the dependence of the α_c relaxation parameters on molecular thickness [4.48, 59, 63]. The magnitude of the relaxation can be calculated from the two site model (sites 180° apart) [4.65].

$$\Delta\kappa'_x = 4f(1 - f)[3\kappa_s/(\kappa_s + \kappa_\infty)][(\kappa_\infty + 2)/3]^2 (N/V) \mu^2/3\varepsilon_o kT) \qquad (4.25)$$

where f is the fraction of dipoles in the ordered site. If U is the energy difference between sites, $f = \exp(-U/kT)/[1 + \exp(-U/kT)]$ and

$$f(1 - f) = \exp(-U/kT)/[1 + \exp(-U/kT)]^2. \qquad (4.26]$$

Since we are measuring a composite of amorphous and crystalline regions we must also use an equation like that for concentrated, nonconducting dispersions [4.66, 67].

$$\frac{\kappa' - \kappa'_x}{\kappa'_\ell - \kappa'_x} \ (\kappa'_\ell \ / \kappa')^{1/3} = 1 - \psi \tag{4.27}$$

In the above equations, κ_s and κ_∞ are the relaxed and unrelaxed relative permittivities for the crystal, $[\Delta\kappa'_x = \kappa_s - \kappa_\infty]$, N and μ are the number per unit volume and the dipole moment of the relaxing units, κ, κ_x and κ_ℓ are the relative permittivities of the sample, crystal and liquid respectively and ψ is the volume fraction of crystals in the sample. Equation (4.27) should be replaced by a more general equation for conducting dispersions [4.68] when necessary. Note from (4.27) that the amplitude of the crystal and liquid relaxations as measured will be considerably smaller than if measured in each phase separately.

It is instructive to consider β phase PVF where we assume a rigid chain of 40 repeat units in the lamellae. 60% of these are nonpolar because of head to head defects and their effective rigid-rod moment will be $16 \times 3.3 \times 10^{-28}$ C·cm. The number per unit volume is $1.8 \times 10^{22}/40$ cm^{-3}, and T = 350 K. The relaxation amplitude is from κ'_x = 3 to 13 [4.61] (remembering Eq. (4.27)). For these conditions, one finds that the fraction of disordered molecules is 8% and U/kT = 2.6. These are quite reasonable values for a crystal with such disordered molecules (30% head to head defects). Now consider U/kT for PVF$_2$ in the same β phase. It will have twice the dipole moment per repeat unit and, with 5% head to head units, 9/4 the number of dipoles for a 40 unit rigid chain. Suppose the energy between the ordered and disordered sites is proportional to the

net difference in the number of fluorines in the sites. Like the dipole moment, the number of fluorines rotated will be 4 1/2 times as great for PVF_2 as for PVF. This gives a value of U/kT of 12 and a disordered fraction of only 10^{-5}. The a_c relaxation amplitude for β phase PVF_2 then is only $(10^{-5}/0.08)(4.5)^2 \approx 10^{-3}$ that of PVF which would not be observable with ordinary dielectric measurements.

4.5.2 Ferroelectricity

PVF_2 in the polar form is often supposed to be a ferroelectric [4.69, 70], which means that it not only is a polar crystal but that the polarity is switchable with an electric field. Direct evidence for a field induced change in the unit cell orientation in PVF_2 measured by x-ray pole figures has been reported [4.21]. Molecular orientation measurements using Raman techniques suffer from the dilution effect of the liquid phase [4.71]. The usual hysteresis measurements of charge vs. field are difficult because of space charge effects and the results are ambiguous. Measurement of piezoelectric [4.11, 30] and pyroelectric [4.72] response as the field is cycled from large positive to negative values does give a hysteresis loop. A poled PVF_2 film was shown to require 450 kV/cm to suppress its piezoelectric response [4.30]. High dielectric constants of the order of 1000 [4.72] are also indicative of ferroelectric switching in β phase PVF_2 but since the same behavior occurs in non-polar α phase PVF_2 as well [4.64], space charge effects are probably dominant.

Polarization vs. time measurements for PVF_2 show two relaxations according to some authors. MURAYAMA et. al. [4.9] report a fast response at less than a second and a slow response at 1-2 hours. FUKADA and OSHIKI [4.73] report the fast response at 1 minute and the slow response at 1 hour. In measurements of pyroelectric response the uniformity of polarization increased significantly when the poling time was increased from 5 to 30 minutes [4.18].

There is disagreement about whether polarization saturates at high temperatures and high fields. MURAYAMA et. al [4.8, 9] reported no saturation for the piezoelectric response in PVF_2 and DAY et. al [4.18] report none for the pyroelectric response (although the data for only uniformly poled samples do show saturation effects) [4.18]. Other data [4.31] shows saturation of the piezoelectric response in PVF_2 and in our laboratory both the piezoelectric and pyroelectric response of VF_2-TFE copolymers saturated as functions of field and temperature [4.39].

Returning again to the calculations of Subsect. 4.5.1, the rigid PVF chain with a moment of 16 x 3.3 x 10^{-28} C·cm when subject to an internal field of 10^6 V/cm (about 4 times the applied field (4.25)) applied in a direction opposite to the crystal moment will reduce the energy difference between the ordered and disordered sites by 2 $\mu E/kT$ to $U_E/kT = 0.6$. Thus in a time of the order of the relaxation time $\tau = (2\pi \times 100 \text{ Hz})^{-1} = 10^{-3}$ sec at 80°C [4.61] a fraction, $f = 1/3$, of the dipoles will reorient to the disordered site thus reducing the energy difference between the sites by 2/3 and making the formerly disordered site the new ordered site. For PVF_2 from the same example U/kT is lowered by 2 $\mu E/kT$ from 12 to $U_E/kT = 3$ so that 5% of the chains would be switched by the field. If this switching lowers U (mean field approximation) by 5% to 11.4, then $U_E/kT = 2.4$ and another 4% will switch lowering U_E/kT further until all molecules switch. In a drawn specimen the molecular axis will be in the plane of the film. Those dipoles which are at 90° to the poling field will not experience as great an energy advantage as a result of switching and perfect alignment is not expected. This situation is similar to that for $BaTiO_2$ where it is shown that a semicrystalline sample achieves only about 1/3 the polarization of the single crystal [Ref. 4.22

p.218]. Both the data and a high field extension of simple dielectric theory support the suggestion that PVF and the β form of PVF_2 are ferroelectric.

4.5.4 Space Charges

Space charge measurements are frequently made by measuring the currents generated by heating, at a uniform rate, a specimen with evaporated electrodes which has previously been cooled under an applied field. The thermally-stimulated short-circuit currents (TSC) result from dipole reorientation and from the change in the dipole moment of the space charge distribution [4.74]. Studies on both amorphous and semicrystalline polymers have shown the space charge to be predominantly positive near the negative poling electrode and negative near the positive poling electrode (heterocharged electret). Kerr effect measurements in liquid nitrobenzene with dc fields show uniform space charge distributions with a net positive charge density of the order of $10^{-8} C/cm^3$ [4.75]. (For a further discussion of such inconsistencies, see Subsect. 1.7.3). Dielectric measurements of PVF and PVF_2 typically show anomalously high values of κ' at high temperatures and low frequencies [4.61, 64, 76]. This effect is generally attributed to ionic space charges [4.64]. It was shown that the interfacial polarization in solid PVF_2 is different from the electrode interfacial polarization effects in liquid PVF_2 and was attributed to space charge polarization at the liquid-crystal interfaces [4.64]. In TSC measurements it was shown that repeated cycling of PVF_2 from 25 to 100°C with an applied field, reduced the space charge effects [4.17]. Space charge concentrations in liquid nitrobenzene [4.75], and the space charge effects seen in dielectric measurements of PVF_2 [4.61, 64, 76] and PVF [4.61] were also reduced by application of dc fields for several hours. This reduction partially recovers with time after removal of the field [4.61, 64, 76].

The general behavior of a conducting liquid with dispersed crystals of roughly equal volume is quite complicated [4.68]. If, as seems likely, ferroelectric switching of the polar cyrstals occurs during the early stages of poling then continued poling results in a flow of charge, mostly through the more conductive liquid phase regions with positive charges moving toward the negative electrode and negative charges toward the positive electrode. At normal poling temperatures (~ 100°C) the current is time dependent and bulk interfacial polarization effects are evident [4.64]. The charge carriers should tend to pile-up at the crystal surfaces where their normal drift is hindered, as shown in Fig. 4.13. This situation is analogous to concentrated emulsions of oil and water [4.67]. TSC results show that space charges are released at temperatures higher than the dipole relaxation maxima and these for PVF_2 are considerably above room temperature [4.74, 77]. As a result, when the specimen is cooled to room temperature the charges are immobilized and remain at the crystal surfaces as in Fig. 4.13. The space charges form a dipole which has the stiffness of the crystal and will produce a piezo and pyroelectric response [see Subsect. 4.2.2]. Note however that the space-charge dipoles if formed from interfacial polarization of the poling-current charges are opposing the molecular dipoles and will reduce the piezo- and pyroelectric response. It is difficult to predict the magnitude of this effect but it will be bigger, the higher the space charge concentration or equivalently the higher the poling current. The observation of a slow poling process reported for PVF_2 [4.9, 30], whereby the piezoelectricity slowly increases with time, and the observation that space charges are removed by dc fields on a similar time scale [4.17, 61, 64, 75, 76], support the idea that a decrease in space charge reduces the masking

effects of space-charge dipoles. Also the partial decay of piezoelectricity with time after removal of the field [4.9] and the partial recovery of space charge density with time [4.61, 76] may be similarly related to the postulated space-charge dipoles.

4.6 Measurements and Data

Piezo- and pyroelectric measurements on polymer films are usually made by applying tension to a strip of polymer and measuring on opposing electrodes the short-circuit charge or open circuit voltage due to a change in the tension. The stress and strain are measured with a load cell and strain gauge and the stress is usually sinusoidal. This basic technique has been discussed previously [4.5, 7]. Measurements can be made by clamping a sample in a vise in series with a load cell. Noise can be reduced for these measurements by the use of good contact electrodes (e.g. evaporated). A double film sandwich with the high potential electrodes together and shielded by the outer grounded electrodes greatly reduces noise problems. Piezoelectric measurements have also been made by applying a field to the specimen and observing the length and thickness changes [4.16], by analyzing the response of a piezoelectric film driven electrically in the neighborhood of its resonant frequencies [4.12] and by applying hydrostatic pressure to the film with He gas [4.33]. Pyroelectric measurements are conveniently made by changing the temperature of the specimen and measuring the charge produced [4.33]. Heating and cooling can be done with a Peltier device [4.78] which is noiser than a heater or, for electromagnetic purposes, with optical radiation [4.19]. The accuracy of piezoelectric data is hard to assess since error analyses are seldom mentioned. Piezoelectric and electrostriction

data on PVF_2 as a function of temperature and frequency has been adequately reviewed previously [4.5, 7, 9].

Applications for polymer transducers or reflectivity measurements [4.79], a photocopy process [4.14], radiation detectors [4.19], night vision targets [4.80], intrusion and fire detectors [4.81], hydrophones [4.82], earphones and speakers [4.10], pressure sensors, strain gauges and many more are being developed or investigated.

4.7 Dipole Model Applied to Semicrystalline Polymers

Eqs. (4.19) and (4.20) can be applied to single crystals of β phase PVF_2. The moment of the crystal will be 13 μC/cm² which gives a polarization of 13 · $(\kappa_\infty + 2)/3 \approx 22$ μC/cm². The linear coefficient of expansion (based on copolymer data) [4.39] and the linear compressibility [4.39] in the polarization direction are about 2×10^{-4}/°C and 2×10^{-10} m²/N. The molecular moment of inertia about the center of mass is $I = 0.7 \times 10^{-45}$ Kgm² and the torsional frequency $\omega_o/2\pi = 2.1 \times 10^{12}$/sec [4.52]. The harmonic approximation gives $\phi° = (kT/I\omega_o^2)^{1/2} = 11.4°$ at room temperature for the rigid rod. Higher order torsional modes will reduce this amplitude so we will assume the polyethylene value [4.29], $\phi = 10°$. Thus, very roughly, for the single crystal (sx),

$$p \ (sx) = 22 \cdot 10^{-6} C/cm^2 \cdot 2 \cdot 10^{-4} \ K^{-1}[3 + 0.03(2 \cdot 2 \cdot 10^{-4} K^{-1} \cdot 350 \ K)^{-1}$$

$$+ \ 3 \cdot 2 \cdot 0.17] = 16 \ nC/cm^2.K$$

(4.28)

$$d \ (sx) = 140 \ pC/N \tag{4.29}$$

The coefficient d_{31} results from the thickness change in the 3 direction due to a stress in the 1 direction,

$$d_{31} \text{ (sx)} = p \ \eta_{31}[\varepsilon_{\infty} + 6\gamma\phi^2]/Y_1 = 120 \text{ pC/N} \tag{4.30}$$

where $\eta_{31} \approx 1/3$ is the assumed Poisson's ratio and $Y_1 = 2 \times 10^9 \text{N/m}^2$ is Young's modulus [4.31].

Ferroelectric ceramic powders in an amorphous polymer matrix were measured [4.83] but not enough details are available to help with the present prediction. The dipole model (Fig. 4.7) can be extended by assuming the Onsager cavity represents an entire crystallite but other assumptions (e.g. no space charges and the sum of the cavity volumes equals the specimen volume) are clearly not valid for the semicrystalline case. However, using the same factor 1/3 for dipole switching efficiency as for $BaTiO_3$ [4.22] and 1/2 for the crystal fraction of the specimen, one gets the results in Table II.

These numbers are close to the highest observed values for drawn polar phase PVF_2. To illustrate further application of the model we return to the calculations of Subsect. 4.5.1 where it was shown that the polarization of PVF_2 is 4 1/2 times that of PVF. Eqs. (4.23) and (4.24) predict that p and d will also be 4 1/2 times greater for PVF_2 than PVF. The highest reported p's for these two polymers are 4.1 nC/K·cm^2 [4.19] and 1 nC/K·cm^2 [4.86] respectively. The ranges of d_{31}'s reported by KAWAI [4.6] for PVF_2 and PVF are 3-7 pC/N and 1-1.3 pC/N respectively.

The model also predicts that the piezoelectric stress constant $e = \eta$ $P[\varepsilon_{\infty} + 6\gamma\phi]$ will vary with orientation and temperature only because of variation in Poisson's ratio η. It is known that e is a strong function of both temperature

and orientation [4.7] beyond the usual variations in η (1/3 to 1/2). These limits do not hold for anisotropic materials such as drawn semicrystalline polymers and direct measurement of η has yet to be made. The predicted ratio of the reduced temperature-induced-strain response p/α to the reduced pressure-induced-strain response d/β is 1.1. This differs significantly from the ratio of 2 typically measured in our laboratory, and is the most serious disagreement with experiment we have yet discovered.

Other models for piezoelectricity in PVF_2 include orientation of dipoles in an anomalous liquid phase [4.87] and increased perfection of the planar zig-zag structures [4.12] both by applied stress. These models are strongly supported by the observation that a strain in the direction of the molecular axes gives a much bigger response than a strain perpendicular to the axes, $d_{31} \approx 5\ d_{32}$ [4.7]. Calculations on the polarization kinetics using several models for PVF_2 have been made [4.88].

4.8 Summary and Conclusions

Some polymers can be made both piezo- and pyroelectric by cooling them in the presence of an applied field. This effect is true piezo- and pyro-electricity rather than electrostriction, conduction, electromechanical effects or the motion of conductors in the field of space charges. Two distinct types of polymers can be piezoelectric. Amorphous polymers are piezo- and pyroelectric by virtue of a non-equilibrium but kinetically stable net dipole orientation. The semicrystalline polymers are piezoelectric due to alignment of polar, ferroelectric crystals dispersed in the amorphous phase. In both types the magnitudes of the piezo- and pyroelectric effects are in accord with the

expected temperature and pressure dependence of the dipolar polarization. Space charges embedded in the polymer normally will not produce a piezo- or pyroelectric current. Those embedded near the crystal-liquid interfaces tend to reduce the piezo- and pyroelectricity. Improved orientation of dipoles and reduction of ionic impurities should increase p and d for PVF_2 by a factor of three above typical values presently reported. The sensitivity of amorphous polymers is limited mainly by dipole moment per unit volume and breakdown strength.

The model presented here was developed along with the writing and was used as a framework for the presentation in order to make the chapter more interesting to the authors and hopefully also for the readers. It is hoped that the model, still largely untested, will provide direction and stimulation for further work in this field.

Acknowledgement

References

4.1   Heaviside, Electrical Papers, Macmillan, London $\underline{1}$, 488 (1892, or Electrical Papers, I. Macmillan, London (1892) p.488.

4.2   M. Eguchi, Phil. Mag. $\underline{49}$, 178 (1925).

4.3   E. P. Adams, J. Franklin Inst., 204, 469 (1927).

4.4   A. Meissner and R. Bechmann, Z. tech Phys. $\underline{9}$, 174, and 430 (1928).

4.5   E. Fukada, Progress in Polymer Science, Japan $\underline{2}$, 329 (1971).

4.6   H. Kawai, Jap. J. Appl. Phys. $\underline{8}$, 975 (1969).

4.7   R. Hayakawa and Y. Wada, Advances in Polymer Science, Springer-Verlag, $\underline{11}$, 1, (1973).

4.8   N. Murayama, J. Polym. Sci., Polym. Phys. Ed., $\underline{13}$, 929 (1975).

4.9   N. Murayama, J. Polym. Sci., Polym. Phys. Ed., $\underline{13}$, 1033 (1975).

4.10   N. Tamura, T. Yamogughi, T. Ayaba and T. Yoshimi, Pioneer Electronic Corp., Reprint No. 986 (G-4) Audio Engineering Society, N.Y. 49th Convention (1974).

4.11   M. Tamura, K. Ogasawara, N. Ono and S. Hagiwara, J. Appl. Phys., $\underline{45}$, 3768 (1974).

4.12   H. Ohigashi, submitted to J. Appl. Phys.

4.13   J. H. McFee, J. G. Bergman, Jr., and G. R. Crane, Ferroelectrics, $\underline{3}$, 305 (1972).

4.14   J. G. Bergman, G. R. Crane, A. A. Ballman and H. M. O'Bryant, Jr., Appl. Phys. Lett., $\underline{21}$, 497 (1972).

4.15   G. Pfister, M. Abkowitz and R. G. Crystal, J. Appl. Phys. $\underline{44}$, 2064 (1973).

4.16   H. Burkard and G. Pfister, J. Appl. Phys. $\underline{45}$, 3360 (1974).

4.17   M. Abkowitz and G. Pfister, J. Appl. Phys. $\underline{46}$, 2559 (1975).

4.18   G. W. Day, C. A. Hamilton, R. L. Peterson, R. J. Phelan, Jr. and L. O. Mullen, Appl. Phys. Lett. $\underline{24}$, 456 (1974).

4.19   R. L. Peterson, G. W. Day, P. M. Gruzensky and R. J. Phelan, Jr., J. Appl. Phys. $\underline{45}$, 3296 (1974).

4.20   R. G. Kepler and P. M. Beeson, Bulletin APS, Series II, $\underline{19}$ 265 (1974)

4.21 R. G. Kepler, E. J. Graeber and P. M. Beeson, Bulletin APS Series II, 20, 350 (1975).

4.22 D. A. Berlincourt, D. R. Curran and H. Jafee, *Physical Acoustics*, Academic Press 1A, 183 (1964).

4.23 T. Furukawa and E. Fukada, Rep. Progs. Polym. Phys. Japan, 16 457 (1973).

4.24 R. E. Collins, Proceedings of the IEEE, 34, 381 (1973).

4.25 G. M. Sessler and J. E. West, J. Acoust. Soc. Am., 53, 1589 (1973).

4.26 L. Onsager, J. Amer. Chem. Soc., 58, 1486 (1936).

4.27 F. I. Mopsik and M. G. Broadhurst, J. Appl. Phys

4.28 E. W. Aslaksen, J. Chem. Phys. 57, 2358 (1972).

4.29 K. Iohura, K. Imade and M. Takayanagi, Polym. J. 3, 357 (1972).

4.30 M. Oshiki and E. Fukada, J. Matls. Sci. 10, 1, (1975).

4.31 E. Fukada and T. Sakurai, Polym. J. 2, 657 (1971).

4.32 R. C. Golike, J. Polym. Sci. 42, 582 (1960).

4.33 M. G. Broadhurst, C. G. Malmberg, F. I. Mopsik, and W. P. Harris in *Electrets, Charge Storage and Transport in Dielectrics*, M. M. Perlman, Ed. The Electrochemical Soc., N.Y. (1973).

4.34 J. Cohen and S. Edelman, J. Appl. Phys. 42, 3072 (1971).

4.35 M. G. Broadhurst, W. P. Harris, F. I. Mopsik and C. G. Malmberg, Polym. Reprints (American Chemical Soc.), 14, 820 (1973).

4.36 W. Reddish, J. Polym. Sci., Part C, No. 14, 123 (1966).

4.37 C. E. Wilkes, V. L. Folt and S. Krimm, Macromolecules, 6, 235 (1973).

4.38 A. von Hipple, Dielectric Matls. and Applications (Technology Press of MIT and John Wiley and Sons, N.Y. 1954).

4.39 G. T. Davis, Special Issue of Anais da Academia Brasileira de Ciencias.

4.40 H. G. Olf, Research Triangle Institute, private communication.

4.41 C. W. Wilson, III, and E. R. Santes, Jr., J. Polym. Sci., Pt.C, <u>8</u>, 97 (1965).

4.42 Von M. Gorlitz, R. Minke, W. Trautvetter and G. Weisgerber, Die Angewandte Makromolekulare Chemie 29/30, 137 (1973).

4.43 J. P. Stallings and S. G. Howell, Polymer Eng. & Sci., <u>11</u>, 507 (1971).

4.44 R. D. Nelson, Jr., D. R. Lide, Jr., and A. A. Maryott, <u>Selected Values of Electric Dipole Moments for Molecules in the Gas Phase</u>, (NSRDS-NBS 10; U.S. Government Printing Office, Washington, D.C.) 1967.

4.45 W. M. Prest, Jr. and D. J. Luca, J. Appl. Phys.

4.46 R. J. Shuford, A. F. Wilde, J. J. Ricca and G. R. Thomas, Nat. Bur. Stand. (U.S.) Interagency Rep. 75-760, pg.59-96 (1975).

4.47 J. B. Lando, H. G. Olf and A. Peterlin, J. Polym. Sci.-A1, <u>4</u>, 941 (1966).

4.48 N. Sasabe, S. Saito, M. Asahina, and H. Kakutani, J. Polym. Sci. A-2, <u>7</u>, 1405 (1969).

4.49 S. Osaki and Y. Ishida, J. Polym. Sci., Polym. Phys. Ed., <u>12</u>, 1727 (1974).

4.50 H. Kakutani, J. Polym. Sci. A-2, <u>8</u>, 1177 (1970).

4.51 E. Fukada and K. Nishiyama, Japanese J. Appl. Phys., <u>11</u>, 36 (1972).

4.52 M. Kobayashi, K. Tashiro and H. Tadokoro, Macromolecules, <u>8</u>, 158 (1975).

4.53 F. J. Boerio and J. L. Koenig, J. Polym. Sci. A-2, <u>7</u>, 1489 (1969).

4.54 G. Natta, G. Allegra, I. W. Bassi, D. Sianese, G. Copoucci, and E. Torti, J. Polym. Sci. Pt.A, <u>3</u>, 4263 (1965).

4.55 S. Osaki and Y. Ishida, J. Polym. Sci., Polym. Phys. Ed., <u>13</u>, 1083 (1975).

4.56 B. L. Farmer, A. J. Hopfinger, and J. B. Lando, J. Appl. Phys., <u>43</u>, 4293 (1972).

4.57 J. B. Lando and W. W. Doll, J. Macromol. Sci., Phys., <u>B2</u>, 205 (1968).

4.58 Kynar 7200, Pennwalt Corp.

4.59 K. Nakagawa and Y. Ishida, J. Polym. Sci., A-2, <u>11</u>, 1503 (1973).

4.60 L. E. Alexander, <u>X-ray Diffraction Methods in Polymer Science</u>, John Wiley, N.Y. (1969).

4.61 S. Osaki, S. Uemura and Y. Ishida, J. Polym. Sci. A-2, 9, 585 (1971).

4.62 A. Peterlin and J. Elwell, J. Matls. Sci., 2, 1 (1967).

4.63 S. Yano, J. Polym. Sci., A-2, 8, 1057 (1970).

4.64 S. Yano, K. Tadano, K. Aoki and N. Koizumi, J. Polym. Sci., Polymer Phys. Ed., 12, 1875 (1974).

4.65 J. D. Hoffman, G. Williams, and E. Passaglia, J. Polym. Sci., Pt.C, No. 14, 173 (1966).

4.66 D. A. G. Bruggeman, Ann. Physik, 24, 636 (1935).

4.67 T. Hanai, N. Koizumi, T. Saigano and R. Gotoh, Kolloid-Zeitschrift, 171, 20 (1960).

4.68 T. Hanai, Kolloid-Zeitschrift, 171, 23, (1960).

4.69 K. Nakamura and Y. Wada, J. Polym. Sci., A-2, 9, 161 (1971).

4.70 J. H. McFee, J. G. Bergman, Jr. and G. R. Crane, Ferroelectrics, 3, 305 (1972).

4.71 G. L. Cessac and J. G. Curro, J. Polym. Sci., Polym Phys. Ed., 12, 695 (1974).

4.72 P. Buchman, Ferroelectrics, 5, 39 (1973).

4.73 E. Fukada and M. Oshiki, Nat. Bur. Stand. (U.S.) Interagency Rep. 75-760, pg. 8-34 (1975).

4.74 J. van Turnhout, Polym. J., 2, 173 (1971).

4.75 E. C. Cassidy, R. E. Hebner, Jr., M. Zahn and R. J. Sojka, IEEE Trans. on Elec. Insulation, 9, 43 (1974).

4.76 S. Uemura, J. Polym. Sci., Polym. Phys. Ed., 10, 2155 (1972).

4.77 J. van Turnhout, Thesis Leiden (1972), TNO Central Laboratoruim Communication, No. 471.

4.78 A. W. Stephens, A. W. Levine, J. Fech, Jr., T. J. Zrebiec, A. V. Cafiero, and A. M. Garofalo, Thin Solid Films, 24, 362 (1974).

4.79 W. R. Blevin and J. Geist, Appl. Opt., 13, 2212 (1974).

4.80 L. E. Garn and E. J. Sharp, IEEE Trans, in Parts, Hybrids and Packaging, PHP10, 28 (1974).

4.81 J. Stern and S. Edelman, U.S. Natl. Bur. Stds. Technical News Bulletin, 56, No.3, 52 (1972).

4.82 James M. Powers, Nat. Bur. Stand. (U.S.) Interagency Rep. 75-760, pg.209 (1975).

4.83 E. Fukada and M. Data, Polym. J., 1, 410 (1970).

4.84 Kureha KF Piezo Element. Measured in our laboratory on sample supplied by N. Murayama.

4.85 Kureha KF Piezo Element. Data supplied by N. Murayama.

4.86 R. J. Phelan, Jr. R. J. Mahler and A. R. Coole, Appl. Phys. Lett., 19, 337 (1971).

4.87 R. Hayakawa, J. Kusuhara, K. Hattori and Y. Wada, Repts. Progr. Polym. Phys. Japan, 16, 477 (1973).

4.88 R. E. Solomon and M. M. Labes, Natl. Bur. Stand. (U.S) Interagency Rep. 75-760, pg.199-209 (1975).

Table 4.1   Polymer identification for Fig. 4.10 according
             to the hydrogen (H) fluorine (F) or chlorine (Cl)
             substituents in sites 1 thru 4.

Polymer	Substituent		
	Hydrogen	Fluorine	Chlorine
Polyethylene (PE)	1,2,3,4		
Polyvinylfluoride (PVF)	1,2,3	4	
Polyvinylidenefluoride (PVF_2)	1, 2	3,4	
Polytetrafluoroethylene (PTFE)		1,2,3,4	
Polyvinylchloride (PVC)	1,2,3		4
Polyvinylidenechloride (PVD_2)	1,2		3,4
Polychlorotrifluoroethylene (PCTFE)		1,2,3	4
Polyacrylonitrile (PAN)	1,2,3	$C \equiv N$ dipole in site 4	

Table 4.2   Estimation of polarization and piezo- and pyroelectric
coefficients for PVF_2 assuming 50% crystallinity and
33% switching efficiency and highest experimental values.

	Estimate	Experimental	Reference
P $(\mu C/cm^2)$	3.7	2–4	[4.11,16,30]
p $(NC/cm^2 \cdot K)$	2.7	4	[4.19]
d $(pC/N$	23	14	[4.84]
d_{31} $(pC/N$	20	20	[4.85]

Figure Captions

Figure 4.1   A diagram of a poling procedure showing the temperature T,
             voltage Φ, time t sequence and the resulting polarization P
             reduced by the permittivity of free space ε_o and applied
             field E_p. The remaining frozen-in reduced polarization is
             the difference between dielectric constants, ε at the two
             temperatures T_r and T_g.

Figure 4.2   A model of an electret with real charges and preferentially
             ordered dipolar charges resulting from the applied voltage Φ.

Figure 4.3   A model of an electret with a sheet of real charge embedded
             in it and induced charges on the short circuited electrodes.
             The σ are the surface charge densities located at the various
             positions, o, x and s.

Figure 4.4   Schematic diagram showing the principles of an electret microphone.

Figure 4.5   A model of a dipolar electret showing the flow of charge resulting
             from a thickness change due to an increase in pressure or a
             decrease in temperature.

Figure 4.6   A model showing how the electret of Fig. 4.5 is used for a pyro-
             electric application. Note the interaction of the film with the
             radiation takes place in the electrode which in turn acts as a
             heat bath.

Figure 4.7   A model for an electret containing a representative dipole of
             moment μ_o, polarizability α, and fixed mean orientation θ with
             respect to the net polarization P.

FIG 4.1

FIG. 4.2

FIG 4.3

FIG. 4.4

Labels in figure:
- METAL PLATE
- NEGATIVELY CHARGED POLYMER FILM
- EVAPORATED METAL ELECTRODE
- R
- R
- COMPRESSIONAL SOUND WAVE

INCREASE IN PRESSURE

OR

DECREASE IN TEMPERATURE

FIG. 4.5

ELECTROMAGNETIC RADIATION

RADIATION ABSORBING
CONDUCTIVE ELECTRODE

FIG. 4.6

ONSAGER CAVITY CALCULATION WITH FROZEN DIPOLES

FIG. 4.7

LOW TEMPERATURE HIGH TEMPERATURE

MEAN DIPOLE MOMENT

RMS FLUCTUATION ANGLE
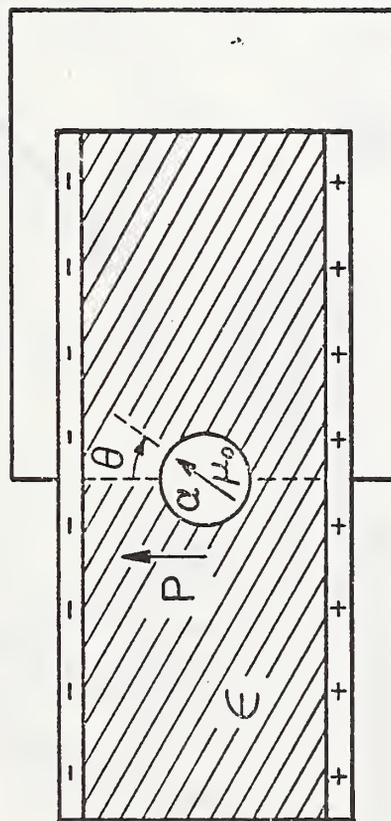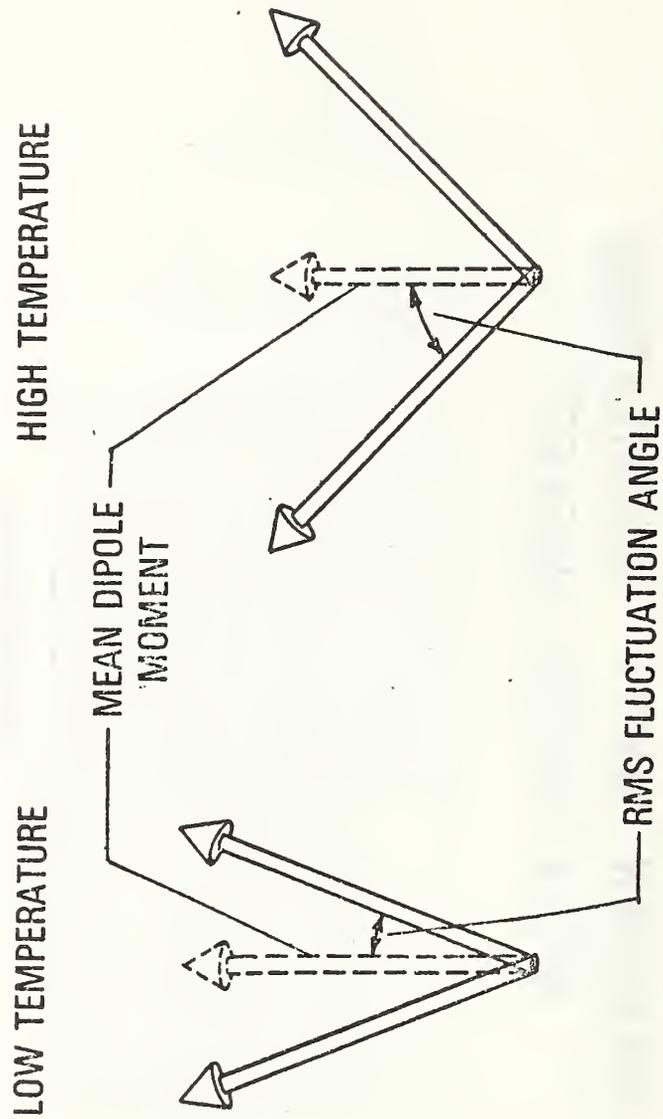
FIG. 4.8

DIRECTION OF POLING FIELD
AND NET ELECTRIC MOMENT

3
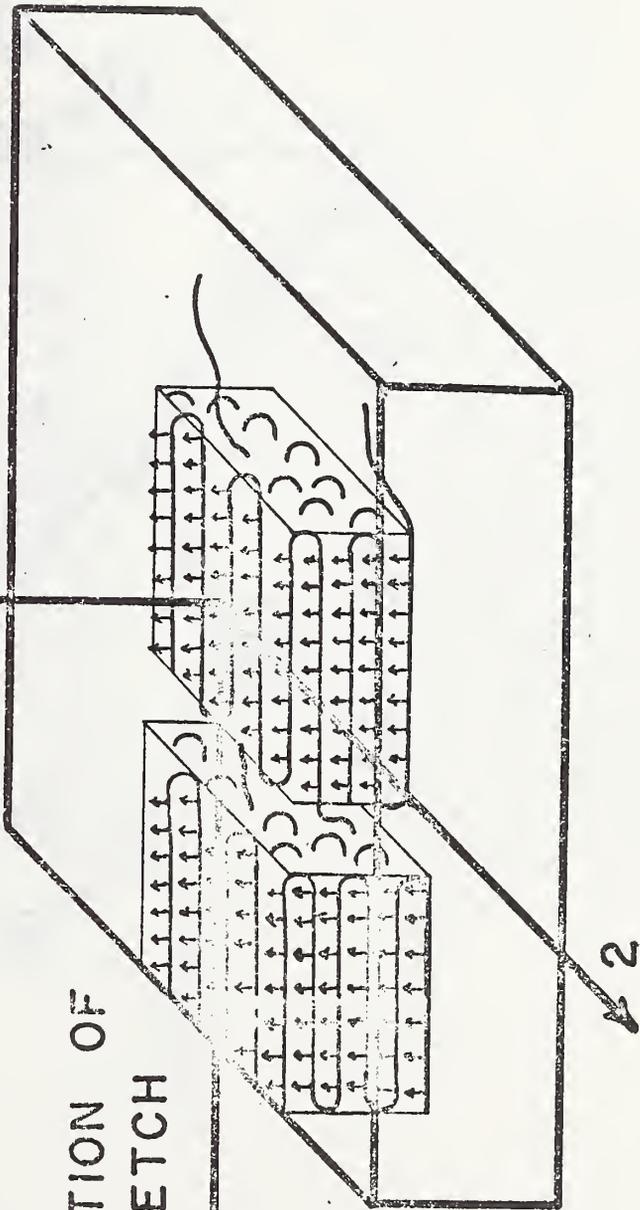
DIRECTION OF STRETCH

1

2

FIG. 4.9
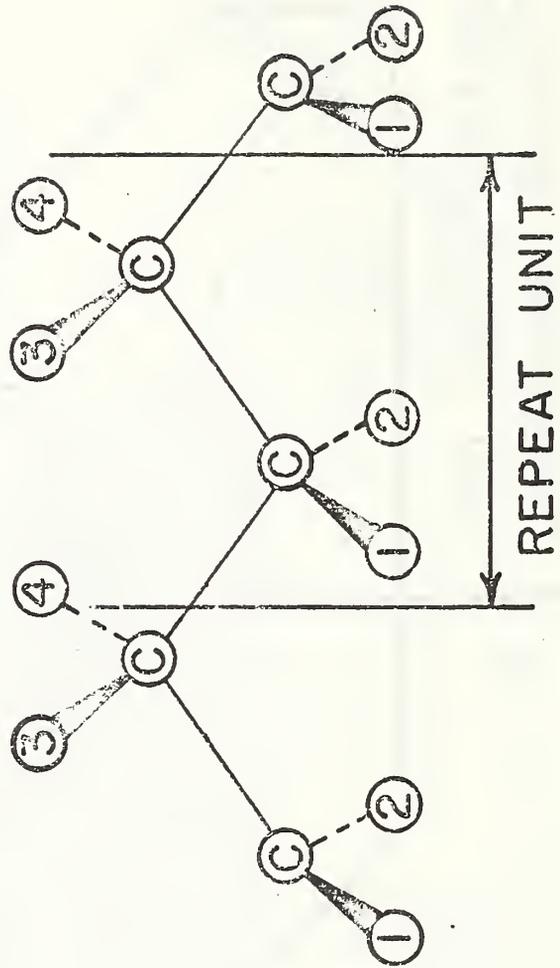
FIG. 4.10

QUENCH CRYSTALLIZED:
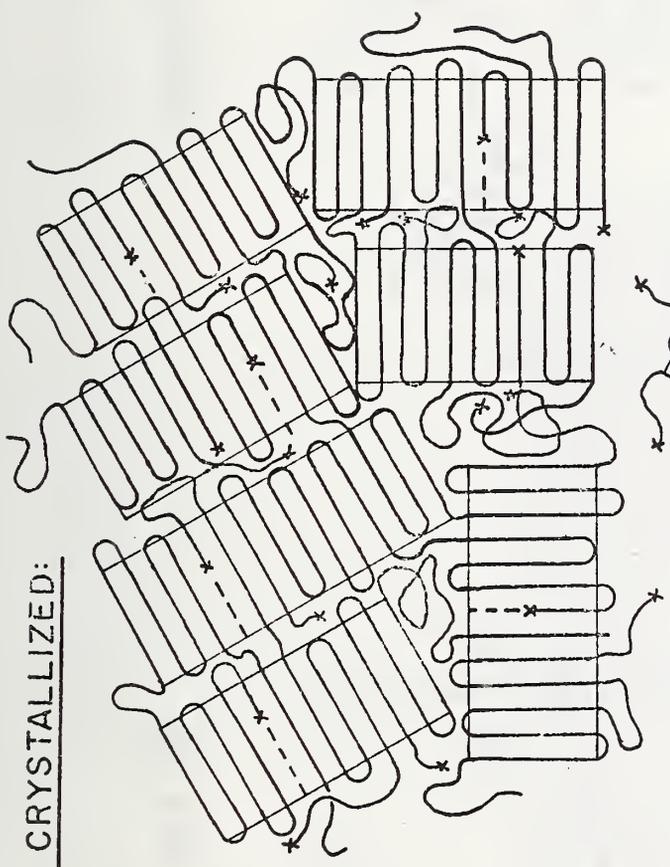
ISOTHERMALLY CRYSTALLIZED:
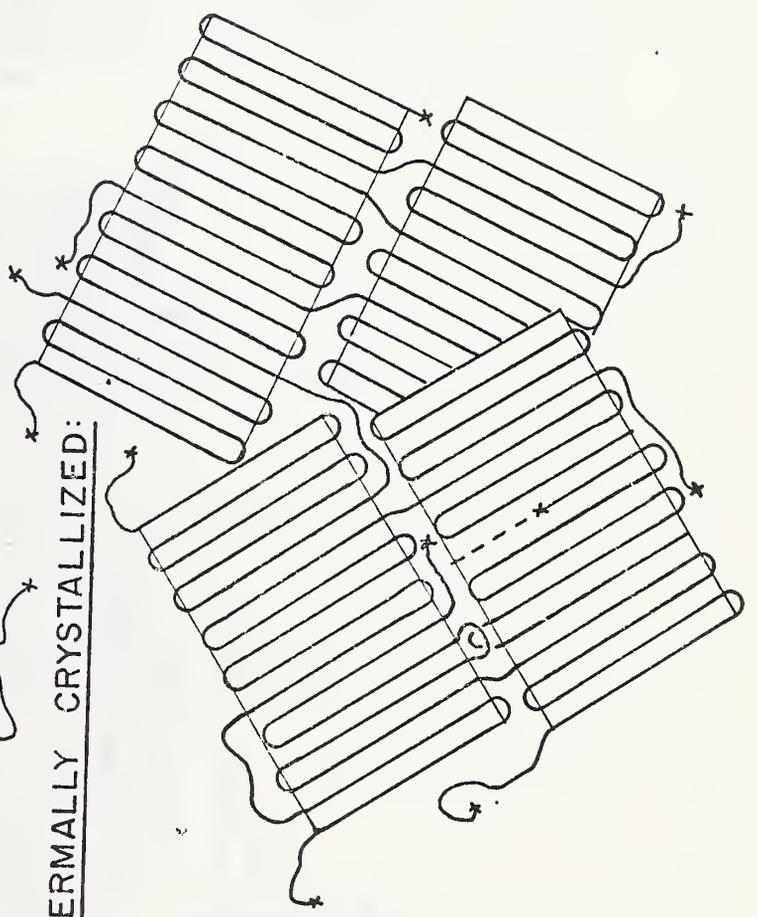
FIG. 4.11
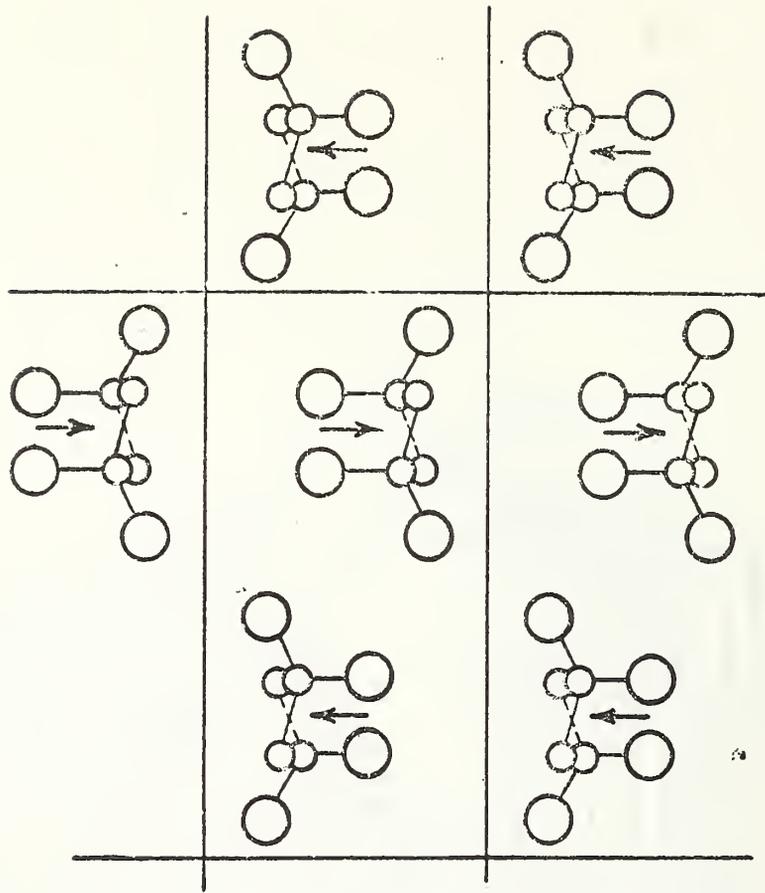
FORM II
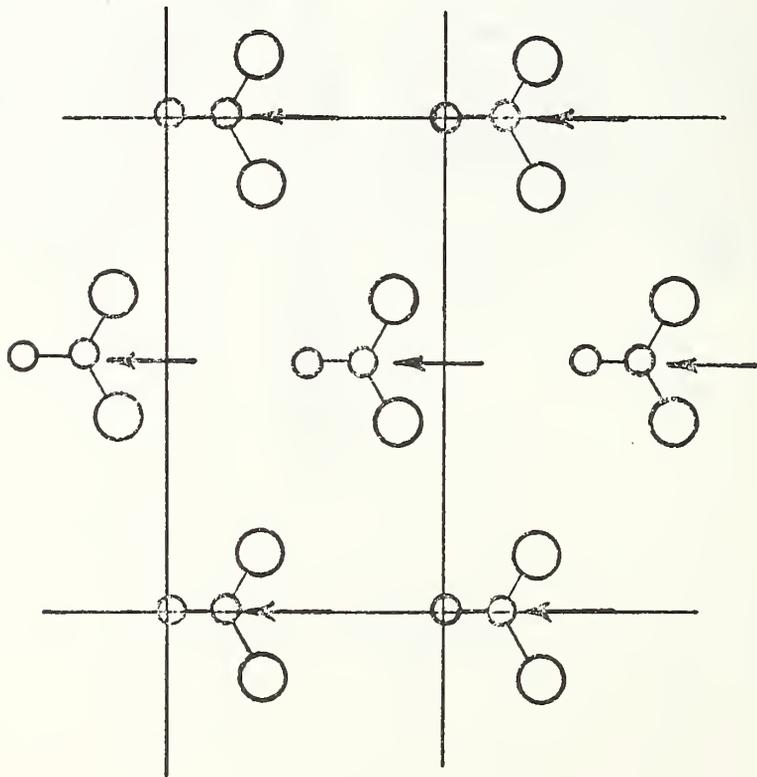
FORMS I and III

FIG. 4.12

FIG. 4.13

U.S. DEPT. OF COMM. BIBLIOGRAPHIC DATA SHEET	1. PUBLICATION OR REPORT NO. NBSIR 75-787	2. Gov't Accession No.	3. Recipient's Accession No.

4. TITLE AND SUBTITLE

Piezo- and Pyroelectric Properties of Electrets

5. Publication Date

October 1975

6. Performing Organization Code

7. AUTHOR(S)

Martin G. Broadhurst and G. T. Davis

8. Performing Organ. Report No. NBSIR 75-787

9. PERFORMING ORGANIZATION NAME AND ADDRESS

NATIONAL BUREAU OF STANDARDS
DEPARTMENT OF COMMERCE
WASHINGTON, D.C. 20234

10. Project/Task/Work Unit No.

11. Contract/Grant No.

12. Sponsoring Organization Name and Complete Address (Street, City, State, ZIP)

Office of Naval Research
Arlington, Va. 22044

13. Type of Report & Period Covered Final
Jan. 1 Dec. 31, 1975

14. Sponsoring Agency Code

15. SUPPLEMENTARY NOTES

16. ABSTRACT *(A 200-word or less factual summary of most significant information. If document includes a significant bibliography or literature survey, mention it here.)*

A model for piezo- and pyroelectricity in polymers is presented. These effects are true piezo- and pyroelectricity rather than electrostriction, conduction, electromechanical effects or the motion of conductors in the field of space charges. Two distinct types of polymers can be piezoelectric. Amorphous polymers are piezo- and pyroelectric by virtue of a non-equilibrium but kinetically stable net dipole orientation. The semicrystalline polymers are piezoelectric due to alignment of polar, ferroelectric crystals dispersed in the amorphous phase. In both types the magnitudes of the piezo- and pyroelectric effects are in accord with the expected temperature and pressure dependence of the dipolar polarization. Space charges embedded in the polymer normally will not produce a piezo- or pyroelectric current. Those embedded near the crystal-liquid interfaces tend to reduce the piezo- and pyroelectricity. Improved orientation of dipoles and reduction of ionic impurities should increase p and d for PVF_2 by a factor of three above typical values presently reported. The sensitivity of amorphous polymers is limited mainly by dipole moment per unit volume and breakdown strength.

17. KEY WORDS *(six to twelve entries; alphabetical order; capitalize only the first letter of the first key word unless a proper name; separated by semicolons)* Electrets; piezoelectricity; polarization; polymers; polyvinylchloride; polyvinylfluoride; polyvinylidenefluoride

18. AVAILABILITY ☒ Unlimited	19. SECURITY CLASS (THIS REPORT)	21. NO. OF PAGES
☐ For Official Distribution. Do Not Release to NTIS	UNCLASSIFIED	54
☐ Order From Sup. of Doc., U.S. Government Printing Office Washington, D.C. 20402, <u>SD Cat. No. C13</u>	20. SECURITY CLASS (THIS PAGE)	22. Price
☒ Order From National Technical Information Service (NTIS) Springfield, Virginia 22151	UNCLASSIFIED	$ 4.25